

NOAA/AVHRR MONITORING OF SNOW COVER FOR MODELLING CLIMATE-AFFECTED RUNOFF IN GANGES AND BRAHMAPUTRA RIVERS

Klaus Seidel and Jaroslav Martinec

*Computer Vision Group, Communication Technology Laboratory, ETHZ
CH 8092 Zürich/Switzerland – email: seidel@vision.ee.ethz.ch*

ABSTRACT

Based on snow cover mapping from NOAA/AVHRR 10-days composites, runoff was modelled in the basins of the rivers Ganges (917'444 km², 0-8,848 m a.s.l.) and Brahmaputra (547'346 km², 0-8,848 m a.s.l.). The temperature and precipitation data were available only as monthly averages and monthly totals, respectively. Another handicap was the relatively small participation of snowmelt in the runoff, evaluated as 9% for Ganges and 27% for Brahmaputra in 1995. Also, the SRM model was encountered with basins of this size for the first time. The combined computed annual runoff for both rivers is 1'009'732·10⁶ m³ as compared with the measured volume of 983'808·10⁶ m³. For a temperature increase of +1.5° and precipitation increase by 10% in the summer, an increase of runoff by nearly 25% was computed for the period from April to September. An increase of the already high flood risk and a reduction of permanent snowfields and glaciers will result should this climate scenario materialize.

INTRODUCTION

The catchment areas of the rivers Ganges (917'444 km²) and Brahmaputra (547'346 km²) have a history of catastrophic floods (Islam and Sado, 2000a). The question arises of how the runoff regime will be influenced by the changing climate. In the framework of the ESA-DUP SPIHRAL Project, year-round NOAA/AVHRR monitoring of the snow cover was carried out. Limited precipitation and temperature data were also provided. The aim of the study was to model the runoff, to evaluate the role of snowmelt and to assess the effect of climate change. New aspects were the large size of the basins and the altitude range from 0 to 8,848 m a.s.l., comprising a variety of climate zones.

Characteristics of the basins

The situation of the basins is shown in Figure 1. The SRM snowmelt runoff model used in this study was originally developed in a basin of only 2.65 km², with terrestrial mapping of the snow coverage. With the advent of remote sensing, it was possible to take up larger and larger basins, as illustrated by several examples in Table 1.



Figure 1: Situation of the basins of the rivers Ganges (G) and Brahmaputra (B) as seen by NOAA/ AVHRR (10-days composite from September 1995)

Table 1: Examples of SRM applications in progressively larger basins

1	Country	Basin	Size [km ²]	Elevation range [m a.s.l.]	Years (seasons)	R ²	D _v %
1	Czech Republic	Modry Dul	2.65	1000 - 1554	2	0.96	1.7
2	Switzerland	Dischma	43.3	1668 - 3146	10	0.86	2.5
3	USA Colorado	South Fork	559	2506 - 3914	7	0.89	1.8
4*	Canada	Illecillewaet	1155	509 - 3150	4	0.86	7.0
5	Chile	Tinguiririca	1460	520 - 4500	1	0.88	0.3
6*	Switzerland	Inn-Martina	1943	1130 - 4049	1	0.82	4.3
7	Morocco	Tillouguit	2544	1050 - 3411	1	0.84	0.5
8*	Switzerland	Rhine-Felsberg	3249	562 - 3425	7	0.70	7.2
9*	USA Colorado	Rio Grande	3419	2432 - 4215	10	0.84	3.8

¹ 1 Martinec, 1963 - 2 Martinec, 1975 - 3 Shafer, 1980 - 4 Rango and Martinec, 1994 - 5 Caceres, 1992 - 6 Baumgartner and Rango, 1995 - 7 Abidi, 1989 - 8 Ehrler, 1998 - 9, 10 Rango and Martinec, 2000 - 11 Kumar et al., 1991 - 12 Sorman, 2001 - 13 Sereno, 1987 - 14 Bedford, 1996

10*	USA California	Kings River	4000	171 - 4341	5	0.82	3.2
11	India	Beas Thalot	5144	1100 - 6400	2	0.80	1.5
12	Turkey	Karasu	10216	1125 - 3487	3	0.95	0.25
13	USA Utah	Sevier	13380	1506 - 3719	1	0.93	4.0
14	Tajikistan	Pyandzh	120534	2141 - 5564	3	0.65	5.6
15*	Bangladesh	Ganges	917444	0 - 8848	1	0.94	8.3

The selected examples represent a wide range of climate. The annual runoff depth amounts to 180 cm in the Modry Dul basin and only to 7 cm in the Sevier basin.

The Himalayan basins have extended the size range by another order of magnitude. It should be noted that data on catchment areas and runoff vary in different publications (for example in Troise and Todd, 1990, Islam and Sado, 2000b). In spite of the smaller catchment area, a higher annual runoff volume is given for Brahmaputra than for Ganges. This discrepancy may be attributed to the different terrain configuration as indicated by the area-elevation curves in Figure 2. For a better comparison, the respective areas are converted to 100 percent. As much as 75% of the Ganges basin is below 500 m a.s.l., compared with only 25% of the Brahmaputra basin. In view of the precipitation altitude gradient, the basin-wide precipitation amounts are higher for Brahmaputra than for Ganges. In addition, precipitation at 1,250 m a.s.l. is higher in the Brahmaputra basin according to the available data.

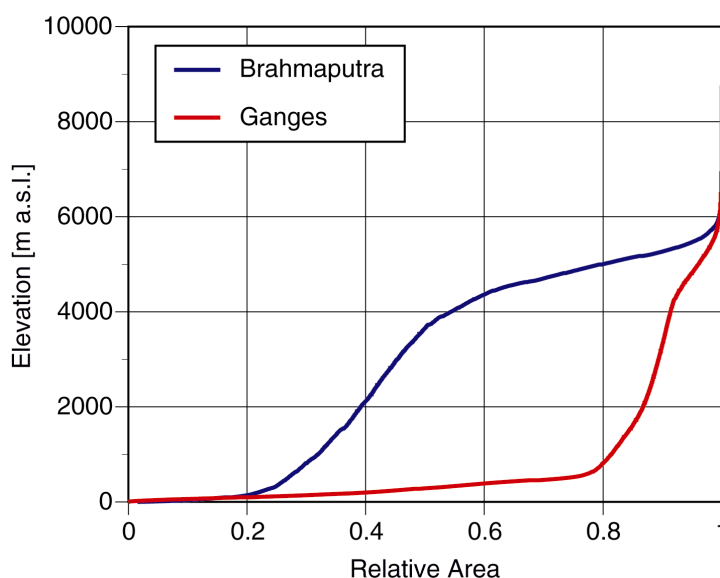


Figure 2: Area-elevation curves for the basins of the rivers Ganges and Brahmaputra

The combined annual runoff volume of Ganges and Brahmaputra amounts to $1,214 \cdot 10^9 \text{ m}^3$ (Troise and Todd, 1990) and passes through Bangladesh to the sea. Consequently, the runoff depth (annual runoff volume divided by area) is extremely high, as illustrated by comparison with several other countries in Table 2. The runoff depth referring to the combined basin areas is within a normal range.

Table 2: Examples of runoff depths for several countries and the world

Country	Area [km ²]	Average annual streamflow 10 ⁹ m ³	runoff depth [m]
Bangladesh	142'776	1'214	8.50
Ganges + Brahmaputra	1'464'790	1'214	0.82
Switzerland	41'290	42.5	1.03
Norway	324'000	405 ²	1.25
France	550'000	183 ^a	0.34
Brazil	8'512'000	9'230 ^a	1.08
Canada	9'975'000	2'470 ^a	0.25
World without antarctica	134'800'000	44'500 ^a	0.33

It should be noted that runoff conditions will be influenced by the respective climate changes in different parts of the world.

Large-scale snow cover mapping

The varying areal extent of the seasonal snow cover is an essential input variable for the SRM model. In view of the large size of both basins, the periodical snow cover mapping had to be based on 10-days composites of NOAA/AVHRR data recorded in 1995. In each month, the best cloud-free composite was selected so that the snow coverage was evaluated in terms of monthly values for the respective elevation zones by means of a digital elevation model (DEM). Both basins were divided into seven elevation zones listed in Table 3.

Table 3: Elevation zones of the basins Ganges and Brahmaputra

Zone	Elevation range [m a.s.l.]	Area Ganges [km ²]	Area Brahmaputra [km ²]
A	0 - 1,000	746'223	178'514
B	1,000 - 2,000	40'359	40'359
C	2,000 - 3,000	24'108	34'357
D	3,000 - 40,000	18'568	50'530
E	4,000 - 5,000	42'736	141'287
F	5,000 - 6,000	32'763	111'777
G	6,000 - 8,848	3'717	2'522
	Total ³	908'474	559'346

Normally, depletion curves of the snow coverage are interpolated from the measured points so that daily values are available for runoff computations. As explained elsewhere (Hall and Martinec, 1985), satellite images showing a short-lived snow cover resulting from preceding snowfalls must

² after Shiklomanov, 1990

³ The areas used in computations slightly deviate from total areas given for the basins.

be disregarded in order to avoid false interpolation of depletion curves. This procedure was not possible in the present case, because dates of summer snowfalls could not be determined. Precipitation data were available only as monthly totals and temperature data only as monthly averages. Therefore the snow coverage is evaluated only as estimated snow covered areas in each month, as illustrated for the Ganges river basin in Figure 3.

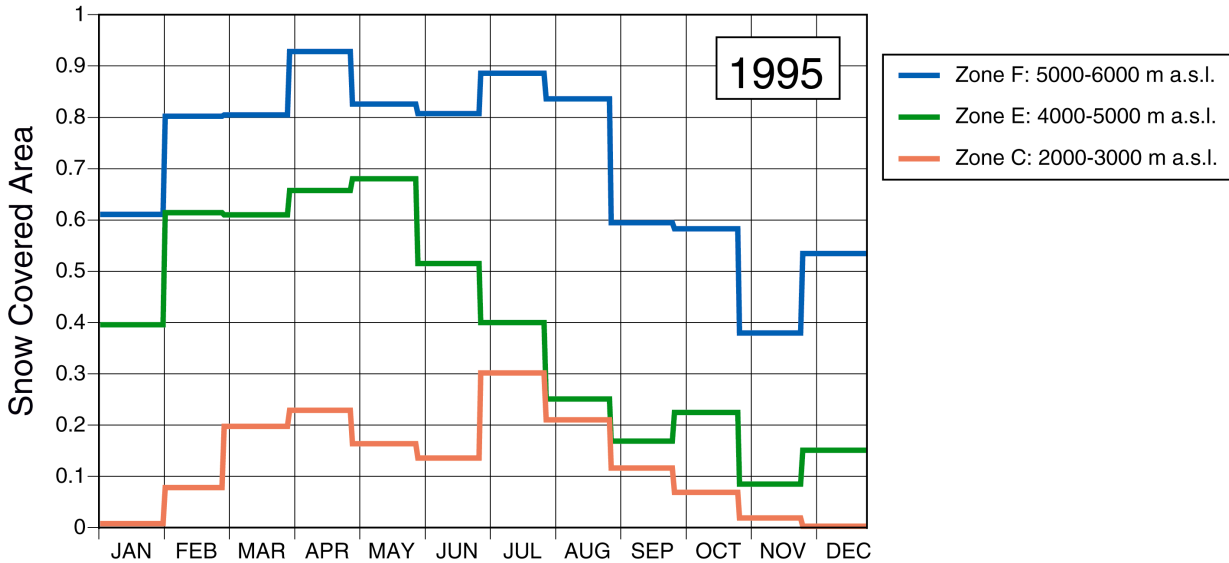


Figure 3: Snow covered areas in the zones C, E, and F of the Ganges river basin in terms of average values for each month, from NOAA/AVHRR data

In both basins, no snow cover was seen by satellites below 2,000 m a.s.l. At this elevation, 50% of precipitation is snow in the Swiss Alps (Dracos, 1980, Seidel and Martinec, in print). The reason is the relatively warmer climate in the Himalayan basins in line with the geographical latitude of 22° - 31°N, as compared with 46° - 47°N for Switzerland.

Runoff modelling

The SRM model is based on the following concept:

(1)
$$Q_{n+1} = I_n (-k_{n+1} + 1) + Q_n k_n :$$

where

- Q = runoff
- I = net input
- k = recession coefficient
- n = sequence of days

Evidently, the recession coefficient k transforms the input (snowmelt + rainfall - losses) into runoff, so that complications with modelling the overland flow, groundwater flow, and flow routing can be avoided. To this effect, the varying values of k must be evaluated as accurately as possible.

An extensive study of the runoff process by environmental isotopes (Dinçer et al., 1970) revealed that k is inversely proportional to the current runoff:

(2)
$$k_{n+1} = x \cdot Q_n^{-y}$$

where

- x, y = constants for the given basin.

The derivation of x, y from historic discharge data is explained elsewhere (Martinec et al., 1998). The model computes k_{n+1} from the already computed Q_n .

Furthermore, the recession coefficient is generally lower (faster recession) in small basins than in large basins, because time runs faster according to Froude’s law of similarity. In basins with insufficient historical discharge data, the constants x, y can be derived indirectly from the size of the basin (Martinec et al., 1998).

In the present case, $x=1.118$ and $y=0.015$. Substituting into Eq. (2), $k=0.953$ for the peak Ganges flow of $42'500 \text{ m}^3\text{s}^{-1}$ in 1995, and $k=0.974$ for the average flow of $9'912 \text{ m}^3\text{s}^{-1}$. Recalling Eq. (1), this means that only 4.7% and 2.6%, respectively, of the daily input leave the Ganges basin within 24 hours, while the rest follows as recession flow. These percentages are correspondingly higher in smaller basins, as shown in Table 4.

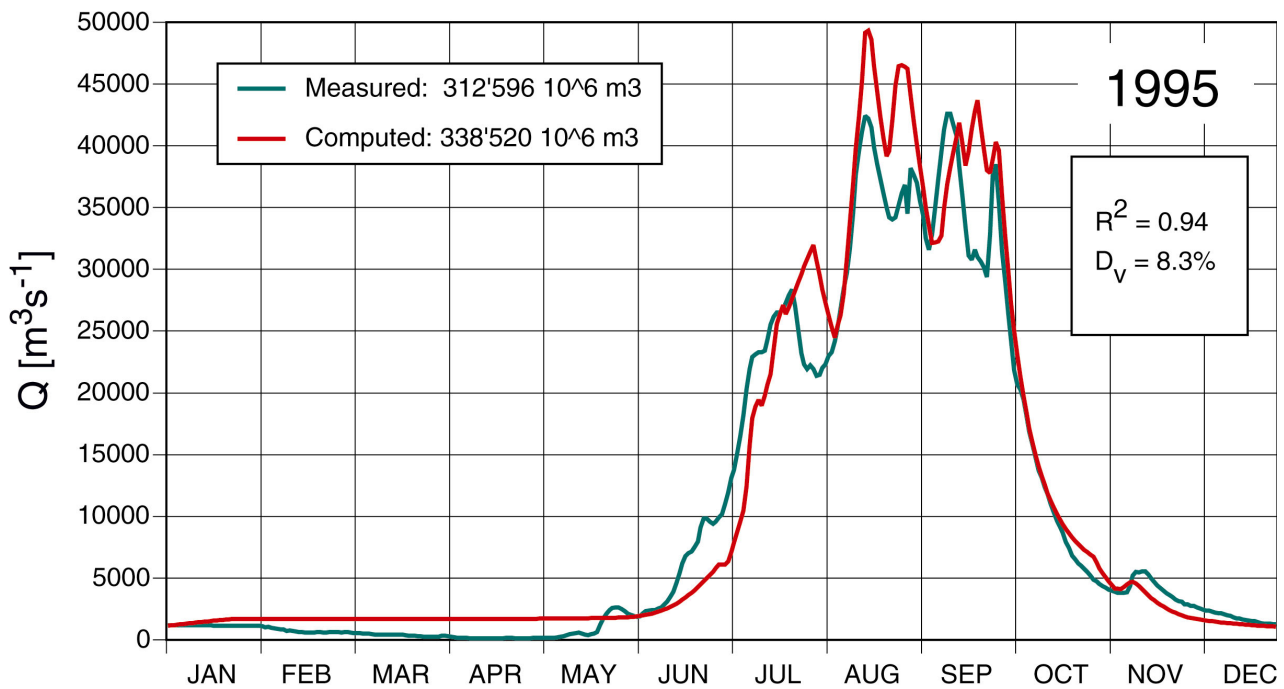


Figure 4: Measured and computed runoff in the river Ganges, 1995

Table 4: Proportions of the immediate outflow from basins of different size

Basin	Area [km ²]	Discharge	Recession coefficient k	Proportion of daily net input leaving within 24 h
Modry Dul	2.65	$Q_{\max}(1967) = 2 \text{ m}^3\text{s}^{-1}$	0.45	55%
Dischma	43.3	$Q_{\max}(1970) = 20 \text{ m}^3\text{s}^{-1}$	0.7	30%
Rhine-Felsberg	3'249	$Q_{\max}(\text{norm}) = 615 \text{ m}^3\text{s}^{-1}$	0.82	18%
Ganges	917'444	$Q_{\max}(1995) = 42'500 \text{ m}^3\text{s}^{-1}$ $Q(1995) = 9'912 \text{ m}^3\text{s}^{-1}$	0.953 0.974	4.7% 2.6%

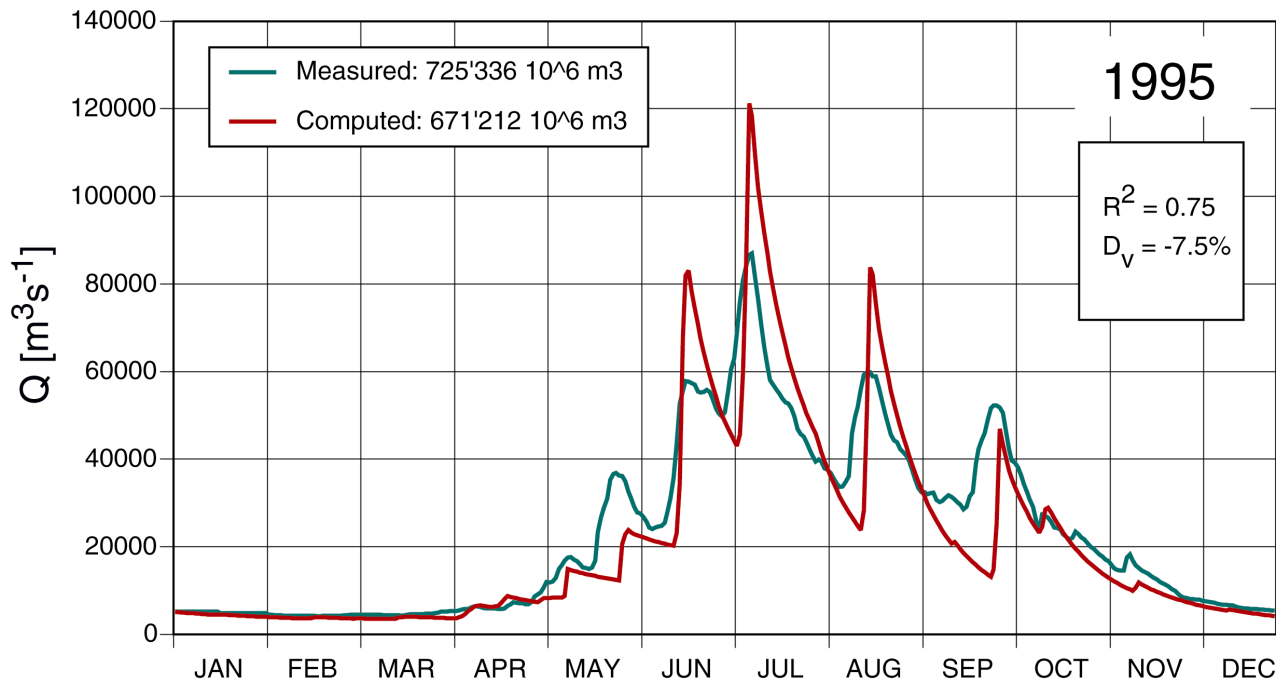


Figure 5: Measured and computed runoff in the river Brahmaputra, 1995

This comparison shows that the model concept automatically takes care of the so-called basin time response, at least of a great part of it.

Another important parameter, the seasonally variable degree-day factor, was preselected in the range of $0.3 - 0.75 \text{ cm}^\circ\text{C}^{-1} \text{ d}^{-1}$. This is slightly higher than degree-day ratios evaluated in the Swiss Alps, because the geographical latitude of the basins and a stronger radiation component is taken into account. The remaining model parameters were in a range similar to that previously found in a smaller Himalayan basin (Kumar et al., 1991): The runoff coefficients c_{snow} from 0.6 to 0.85, c_{rain} from 0.5 to 0.7, critical temperature (snow/rain) from 0.75 to 2°C . The temperature lapse rate was slightly lower than usual, 0.6°C per 100 m, as indicated by satellite images of the snow cover at different altitudes. Runoff simulations are shown in Figure 4 and Figure 5.

In the SPIHRAL Interim Report (Baumgartner, 1999), monthly precipitation totals were empirically disaggregated, taking into account the statistically determined numbers of precipitation events in each month and the timing of peak flows. Uniform daily temperatures in each month had to be used.

In view of these deficiencies and of the unprecedented properties of the basins, the runoff simulations may be considered acceptable.

From day-to-day runoff computations, the proportions of the respective runoff components can be totalized, as graphically illustrated in Figure 6 and Figure 7. The participation of snowmelt in the runoff in the Ganges river basin is much smaller than in the Brahmaputra river basin: 9.3% including 1.1% from new snow against 26.6% including 2.6% from the new snow. This difference is explained by the shape of area-elevation curves in Figure 2. From the satellite imagery, snow occurs above 2,500 m a.s.l., which represents 57% of the Brahmaputra basin and only 12% of the Ganges basin. Almost the whole snowmelt contribution to runoff occurs in April through August. It also includes icemelt, because glaciers could not be mapped separately. The new snow (temporary snowfalls) refers to the hitherto snow-free areas, while the remaining part is integrated into the seasonal snow cover. It is, however, difficult to properly identify temporary snowfalls because of inadequate temperature and precipitation data. Proportions of the input components can also be evaluated separately for each elevation zone (Seidel and Martinec, in print).

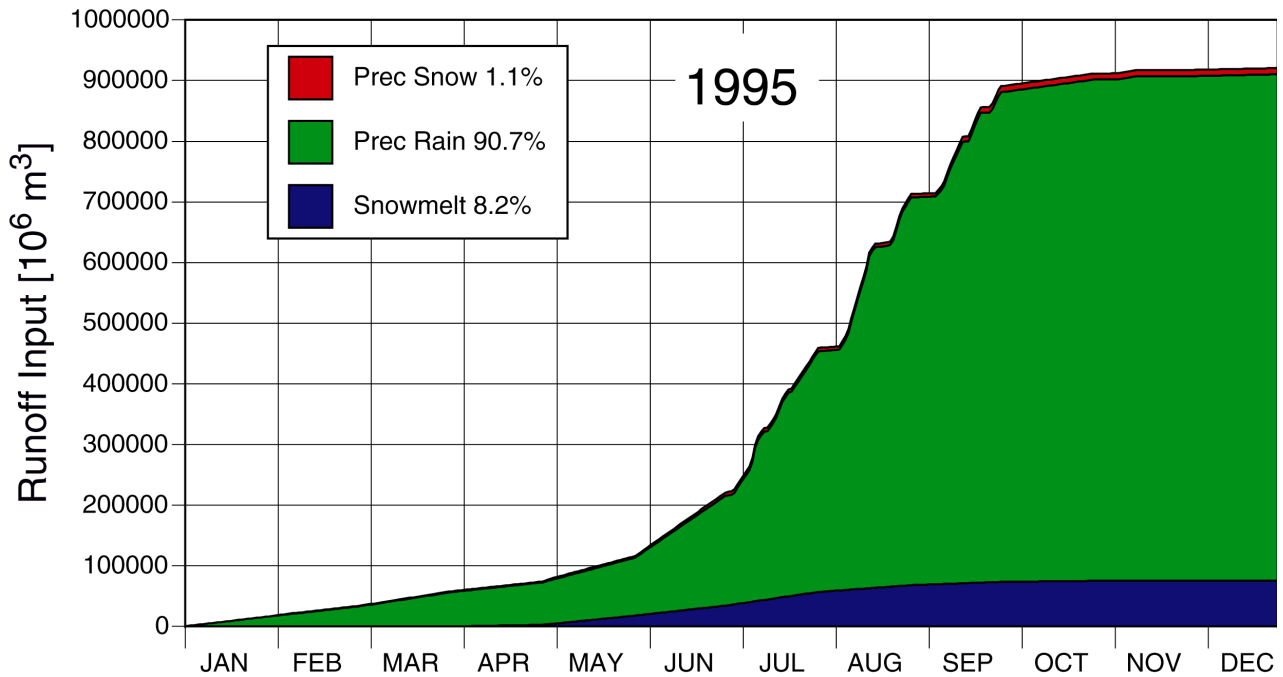


Figure 6: Cumulative curves of the computed daily snowmelt depths, rainfall depths, and melted precipitation in the form of snow in the Ganges basin

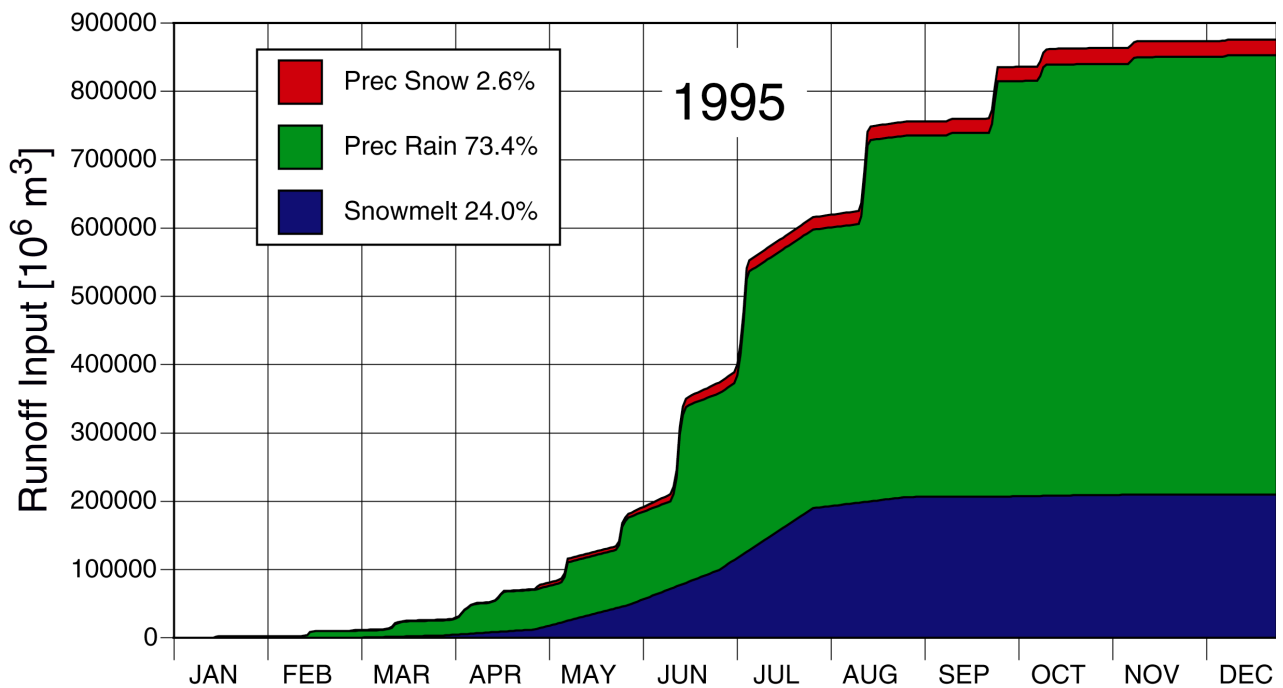


Figure 7: Cumulative curves of the computed daily snowmelt depths, rainfall depths and melted precipitation in the form of snow in the Brahmaputra basin

Effect of climate change on snow cover and runoff

At present times, hydrological studies have a limited validity, because the global warming is in progress. It is therefore advisable to complement such evaluations with predictions of future conditions resulting from assumed climate scenarios. This is particularly important for the rivers Ganges and Brahmaputra because of the high flood risk. By way of example, Figure 8 shows predicted changes of temperature and precipitation for the year 2030 in five different areas of the

world (see Table 5) according to the Intergovernmental Panel on Climate Change, IPCC (Jäger and Ferguson, 1991).

Table 5: Estimates for climate changes by the year 2030

Region	Temperature		Precipitation		Soil moisture
	Winter	Summer	Winter	Summer	Summer
1 Central North America	+2 to +4°	+2 to +3°	0 to 15%	-5 to -10%	-15 to -20%
2 Southern Asia	+1 to +2°	+1 to +2°		+5 to +15%	+5 to +10%
3 Sahel	+1 to +3°	+1 to +3°			
4 Southern Europe	+2°	+2 to +3°		-5 to -15%	-15 to -25%
5 Australia	+2°	+1 to +2°		+10%	

As the general circulation models are further developed, the climate change scenarios are being updated and revised. It has been pointed out on several occasions (Klemes, 1985, Becker and Serban, 1990, Nash and Gleick, 1991, McCabe and Hay, 1995) that calibration models are not suitable for evaluations of the effect of climate change on runoff. As a non-calibration model, SRM (WINDOWS version) can take up changes of temperature and precipitation referring to a year, to months and days, if such detailed scenarios become available. In the present study, a temperature increase of +1.5°C, a precipitation increase of 10% in the summer, and an increase of humidity by 5 to 10% in the summer was assumed.



Figure 8: Estimates for climate changes in different parts of the world

The climate-affected hydrographs are shown in Figure 9 and Figure 10 in comparison with the simulated runoff for the year 1995.

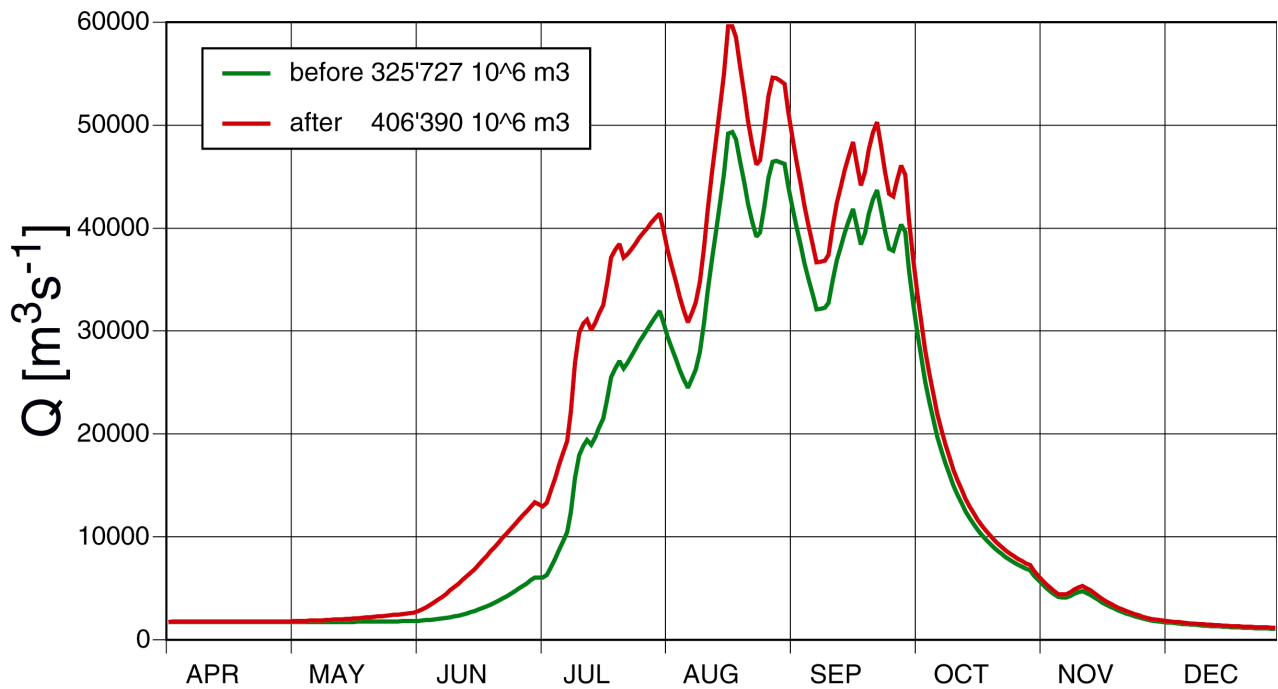


Figure 9: Computed (1995) and climate-affected runoff in the basin of Ganges

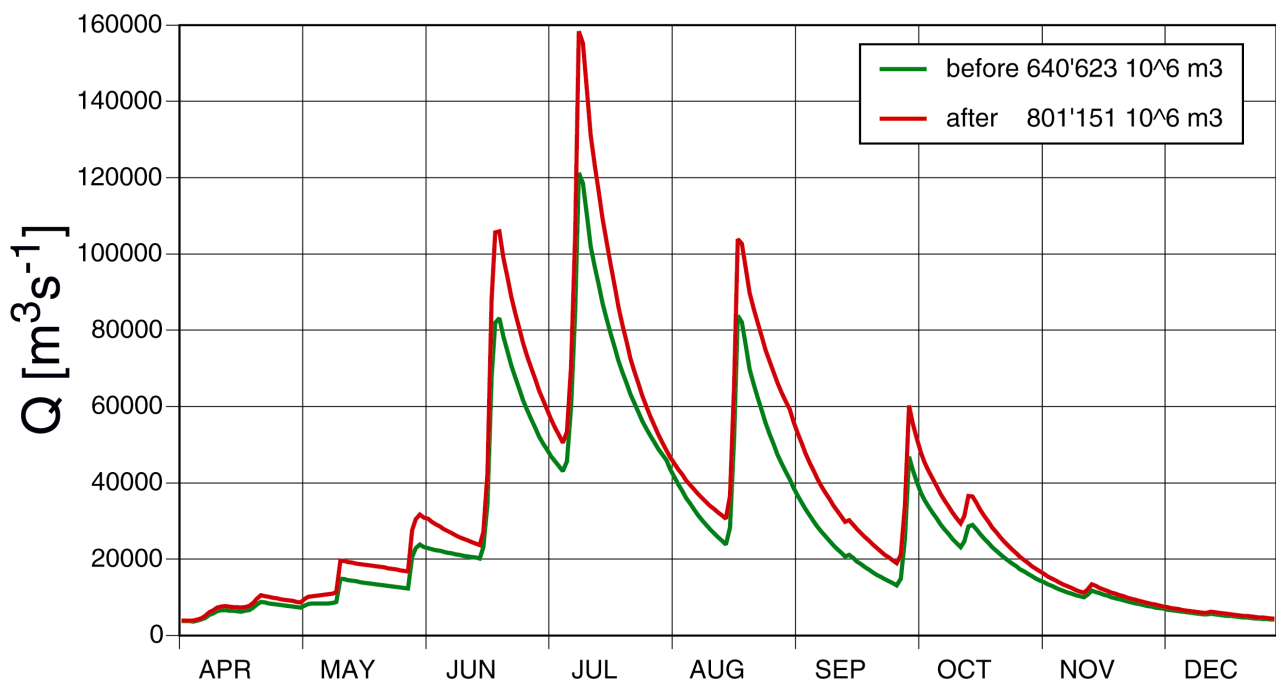


Figure 10: Computed (1995) and climate-affected runoff in the basin of Brahmaputra

New temperatures ($T+1.5^{\circ}\text{C}$) and precipitation ($P \times 1.1$ in the summer) have been substituted, changed snow cover areas and the runoff coefficient for rain increased by 5% in the summer. The period extends from April to December so that the runoff volumes “before” are correspondingly smaller than those computed in Figure 4 and Figure 5.

In both basins, the yearly runoff volume is nearly by 25% higher than in 1995. The increase exceeds the effect of higher precipitation and reduced losses by evapotranspiration. An explanation is

provided by Figure 3: The seasonal snow cover has not been completely melted by the end of the annual cycle in the elevation zones E and F. Consequently, additional runoff resulted from melting of glaciers and permanent snowfields by higher temperatures.

An increase of the summer peak flows is also to be expected. In 1988, the peak daily discharge of the Brahmaputra river was $99'500 \text{ m}^3\text{s}^{-1}$ and $72'300 \text{ m}^3\text{s}^{-1}$ for the Ganges (Islam and Sado, 2000a). In 1995, the respective values were $87'000 \text{ m}^3\text{s}^{-1}$ and $42'600 \text{ m}^3\text{s}^{-1}$, as shown in Figure 4 and Figure 5. The climate-affected peaks in Figure 9 and Figure 10 are by 20-30% higher than the computed peaks. However, the absolute values must be disregarded, because the computed peaks are higher than the measured ones due to the inaccurate simulations.

CONCLUSIONS

The application of remote sensing in hydrology and the limits of runoff modelling have been extended in several ways:

1. The order of magnitude of mountain basins in which runoff can be modelled has been extended to $1'000'000 \text{ km}^2$ and the elevation range to 8,800 m.
2. 10-days composites of NOAA/AVHRR images of the snow cover can be used as the model input variable in very large basins.
3. Once the runoff has been modelled, it is automatically possible to evaluate the effect of any climate change scenario on the seasonal snow cover and runoff.

With daily temperature and precipitation data instead of just monthly values, it would be possible to evaluate the snow and runoff conditions in a changed climate more accurately.

Satellite monitoring is the only efficient method to keep track of the changing seasonal snow cover and glaciers, particularly in large remote sensing areas like those in the present study.

REFERENCES

1. Abidi, A. (1989). Martinec-Rango snowmelt runoff model applied to the Tillougit basin of Morocco. Master's thesis, South Dakota School of Mines and Technology, Rapid City, South Dakota, USA.
2. Baumgartner, M. F. (1999). Snowmelt runoff modeling in the Ganges and Brahmaputra river basins. Interim Report ESA-DUP Project SPIHRAL.
3. Baumgartner, M. F. and Rango, A. (1995). A Microcomputer-Based Alpine Snow-Cover Analysis System (ASCAS). *Photogrammetric Engineering & Remote Sensing*, 61(12):1475–1486.
4. Becker, A. and Serban, P. (1990). Hydrological models for water resources system design and operation. WMO Operational Hydrological Report 34, World Meteorological Organization, Geneva.
5. Bedford, D. (1996). (private communication).
6. Causeries, F. E. (1992). Aplicacion del modelo "SRM 3-11" en cuencas de los Andes Centrales. In *Secundas Jornadas de Hidraulica* Francisco Javier Dominguez, pages 283–295. Departamento di Hidrologia Ministerio de Obras Publicas, Santiago, Chile.
7. Dinçer, T., Payne, B., Martinec, J., Tongiorgi, E., and Florkowski, T. (1970). Snowmelt runoff from measurements of tritium and oxygen-18. In *Water Resources Research (AGU)*, volume 6, pages 110–124.
8. Dracos, T. (1980). *Hydrologie*. Springer Verlag, Wien, New York, p. 39.

9. Ehrler, C. (1998). Klimaänderung und alpine Schneedecke – Auswirkungen auf das Abflussregime am Beispiel des Einzugsgebiets 'Rhein-Felsberg'. vdf Hochschulverlag an der ETH Zürich, NFP 31 Schlussbericht. 117 pages.
10. Hall, D. K. and Martinec, J. (1985). Remote Sensing of Ice and Snow. Chapman and Hall, London - New York, 189 pages.
11. Islam, M. M. and Sado, K. (2000a). Flood hazard assessment in Bangladesh using NOAA/AVHRR data with geographical information system. *Hydrological Processes*, 14:605–620. John Wiley & Sons Ltd.
12. Islam, M. M. and Sado, K. (2000b). Satellite remote sensing data analysis for flood damaged zoning with GIS for flood management. *Annual Journal for Hydrologic Engineering, JSCE*, 44:301–306.
13. Jaeger, J. and Ferguson, H. L., editors (1991). *Climate Change: Science, Impacts and Policy*, chapter Proceedings of the Second World Climate Conference, Geneva, Switzerland, page 35. Cambridge University Press, Cambridge, UK.
14. Klemes, V. (1985). Sensitivity of water resources systems to climate variations. WCP Report 98, World Meteorological Organization, Geneva.
15. Kumar, V., Haefner, H., and Seidel, K. (1991). Satellite snow cover mapping and snowmelt runoff modelling in Beas basin. In XX General Assembly IUGG in Vienna 1991, IAHS-IUFRO Symposium Snow, Hydrology and Forests in High Alpine Areas, pages 101–109. IAHS Publication No. 205.
16. Martinec, J. (1963). Forecasting streamflow from snow storage in an experimental watershed. In *Surface Waters*, pages 127–134. IAHS Publ. No. 63.
17. Martinec, J. (1975). New methods in snowmelt-runoff studies in representative basins. In IAHS Symposium on Hydrological Characteristics of River Basins, pages 99–107. IAHS Publ. No. 117.
18. Martinec, J., Rango, A., and Roberts, R. (1998). *Snowmelt Runoff Model (SRM) User's Manual*. Geographica Bernensia P 35, Department of Geography—University of Bern.
19. McCabe, G. J. J. and Hay, L. E. (1995). Hydrological effects of hypothetical climate change in the East River basin, Colorado, U.S.A. *Hydrological Sciences Journal*, 40(3):303–318.
20. Nash, L. L. and Gleick, P. H. (1991). Sensitivity of streamflow in the Colorado basin to climatic changes. *Journal of Hydrology*, 125:221–241.
21. Rango, A. and Martinec, J. (1994). Model accuracy in snowmelt-runoff forecasts extending from 1 to 20 days. *AWRA Water Resources Bulletin*, 30(3):463–470.
22. Rango, A. and Martinec, J. (2000). Hydrological effects of a changed climate in humid and arid mountain regions. *World Resources Review*, 12(3):493–508.
23. Seidel, K. and Martinec, J. (in print). Snowmelt contributions to runoff in an extremely wide altitude range from large area satellite imagery. In 5th International Workshop on The Applications of Remote Sensing in Hydrology, October 2-5, 2001, Montpellier, FRANCE.
24. Sereno, D. J. (1987). Applying the Martinec-Rango Snowmelt Runoff Model with Landsat satellite data imaging techniques: An alternative method of streamflow prediction in Utah's Wasatch Mountains. Master's thesis, Dept. of Civil Engineering, Brigham Young University, Provo, Utah, USA.
25. Shafer, B. A. (1980). Report on the Martinec model project. Technical Report, USDA Soil Conservation Service, Denver Colorado.
26. Shafer, B. A., Jones, E. B., and Frick, D. M. (1981). Snowmelt runoff simulations using the Martinec-Rango model on the South Fork Rio Grande and Conejos river in Colorado. AgRISTARS Report CP-G1-04072, Goddard Space Flight Center, Greenbelt, Md.

27. Shiklomanov, I. A. (1990). Global water resources. *Natures and Resources*, 26(3):343–43.
28. Sorman, U., Uzunoglu, E., and Kaya, H. I. (2000). Application of the SRM and SLURP models in eastern Turkey using remote sensing and geographical information systems. In *Remote Sensing and Hydrology 2000. Proceedings of the Santa Fe Symposium, April 2000*, IAHS Publ. No. 267, pages 81–86.
29. Troise, F. L. and Todd, D. K. (1990). *The Water Encyclopedia*. Lewis Publishers, Inc., 121 South Main Street, Chelsea, Michigan, USA.